

Three-Coordinate Copper(I) Amido and Aminyl Radical Complexes

Neal P. Mankad,[†] William E. Antholine,[‡] Robert K. Szilagy,^{*,§} and Jonas C. Peters^{*,†}

Department of Chemistry, Massachusetts Institute of Technology, Cambridge, Massachusetts 02139, Department of Biophysics, Medical College of Wisconsin, Milwaukee, Wisconsin 53226, and Department of Chemistry and Biochemistry, Montana State University, Bozeman, Montana 59717

Received December 18, 2008; E-mail: szilagy@montana.edu; jcpeters@mit.edu

Electron transfer (ET) through proteins often utilizes copper-containing active sites as efficient one-electron relays. The type-1 active sites of the blue copper proteins are prominent examples.^{1–3} It is generally thought that high ET rates through type-1 redox sites occur because the protein environments enforce unusual trigonally distorted coordination spheres to allow for minimal structural reorganization during ET.^{1,4} Though large Cu^{II}/Cu^I self-exchange ET rate constants (k_s) in the range observed for type-1 sites have been achieved in certain synthetic monocopper systems using geometries distinct from trigonal environments,⁵ ET studies have yet to be conducted in a synthetic system featuring isolated, trigonally disposed copper centers. The simplest such systems would contain a trigonal planar geometry.

Here we report the structural characterization of a trigonal planar system featuring formally Cu^{II} and Cu^I amido complexes related by a reversible one-electron redox event. We find in this system that ET is extremely rapid and is accompanied by a small degree of structural reorganization during redox. We propose that this structural rigidity in the absence of secondary coordination sphere effects results from significant covalency of the copper–amide linkages. In fact, a Cu^I–aminyl radical description of the formally Cu^{II}–amide complex may be most appropriate.

The anionic Cu^I amido complex $\{[\text{Ph}_2\text{BP}^{\text{Bu}_2}]\text{Cu}(\text{NTol}_2)\}\{\text{Li}(12\text{-crown-4})_2\}$ (**1**) ($[\text{Ph}_2\text{BP}^{\text{Bu}_2}] = \text{Ph}_2\text{B}(\text{CH}_2\text{P}^{\text{Bu}})_2$, Tol = *p*-tolyl) was synthesized by the reaction between $[\text{Ph}_2\text{BP}^{\text{Bu}_2}]\text{Cu}(\text{pyridine})$ and LiNTol_2 in the presence of excess 12-crown-4⁶ and isolated as a yellow, diamagnetic solid. The cyclic voltammogram of **1** features a fully reversible redox event at -0.882 V versus $\text{FeCp}_2^+/\text{FeCp}_2$ (Figure S1 in the Supporting Information). Chemical oxidation of **1** with $[\text{FeCp}_2][\text{B}(3,5\text{-(CF}_3)_2\text{C}_6\text{H}_3)_4]$ produced paramagnetic $[\text{Ph}_2\text{BP}^{\text{Bu}_2}]\text{Cu}(\text{NTol}_2)$ (**2**) as red needles with optical bands at 365 nm ($\epsilon = 870 \text{ M}^{-1} \text{ cm}^{-1}$) and 480 nm ($\epsilon = 600 \text{ M}^{-1} \text{ cm}^{-1}$).

Both **1** and **2** were studied by single-crystal X-ray crystallography (Figure 1; also see Figures S2 and S3). Immediately evident upon comparison of the two oxidation states is the minimal degree of structural rearrangement at the Cu centers upon ET (see Figure 1B for an overlay). In both structures, the Cu centers have rigorously planar coordination geometries [$\Sigma\angle = 359.97(14)^\circ$ for **1** and $359.97(17)^\circ$ for **2**]. The Cu–P distances, P–Cu–P angles, and P–Cu–N angles are all essentially identical in both **1** and **2**. The most notable structural difference is the Cu–N contraction seen upon oxidation from **1** [2.0019(18) Å] to **2** [1.906(2) Å]. The UV–vis spectra of **2** in benzene and acetonitrile are identical (Figure S5), consistent with **2** being three-coordinate in solution as well as in the solid state. A series of trigonal planar β -diketimino

nato Cu^{II} complexes synthesized by Tolman and co-workers⁷ remain the only other reported examples of three-coordinate, formally Cu^{II} complexes.

Taken together, complexes **1** and **2** represent the only three-coordinate copper system to be isolated and structurally characterized in two distinct redox states.⁸ Therefore, it was of interest to study the **2/1** self-exchange ET rate constant k_s . As discussed in the Supporting Information, we determined that k_s in this system is too large to measure accurately by NMR line width analysis, implying a lower limit of $k_s \geq 10^7 \text{ M}^{-1} \text{ s}^{-1}$.⁹ For comparison, blue copper proteins typically exhibit k_s values on the order of $10^6 \text{ M}^{-1} \text{ s}^{-1}$.¹

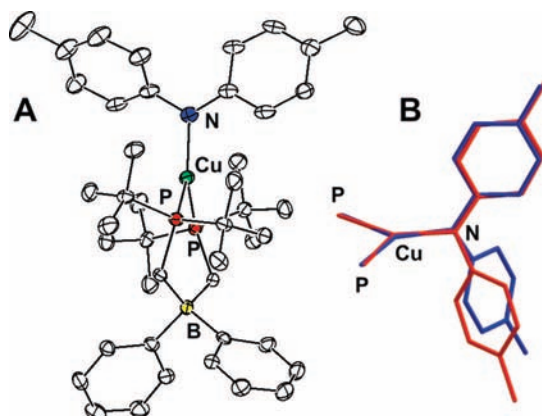


Figure 1. (A) Solid-state structure of **2**. (B) Structural overlay of anion **1** (red) and neutral **2** (blue), with only the phosphorus atoms of $[\text{Ph}_2\text{BP}^{\text{Bu}_2}]$ shown.

Spectroscopic studies of the dinuclear Cu_A ET sites in cytochrome *c* oxidase and nitrous oxide reductase have revealed significant covalency in the Cu₂(μ -SR)₂ cores, resulting in significant sulfur-centered redox during ET.¹⁰ This covalency likely contributes to the extremely efficient ET rates mediated by Cu_A,¹¹ and this concept has been discussed in the context of synthetic Cu₂(μ -X)₂ model complexes.^{9,12} It is also likely that such Cu–ligand covalency likewise plays a role in the functional properties of the type-1 active sites in blue copper proteins.¹¹ We therefore sought to probe the intimate electronic structures of **1** and **2**, in particular questioning whether oxidation of the amido ligand occurs during the interchange of **1** and **2**. In other words, we wondered if the Cu^I–aminyl radical form of **2** is an important resonance contributor. A Rh complex synthesized by Grützmacher and co-workers in 2005 was the first reported example of an isolable 1:1 aminyl radical complex of a transition metal,¹³ and unlike their aryloxy radical analogues, such complexes remain quite rare.¹⁴ To our knowledge, examples of nonchelated aminyl radical ligands have not been reported to date.

Cu K-edge X-ray absorption spectroscopy (XAS) was used to probe the effective Cu oxidation states in **1** and **2**. The Cu K-edge

[†] Massachusetts Institute of Technology.

[‡] Medical College of Wisconsin.

[§] Montana State University.

spectra for **1** and **2** in Figure 2A show a high degree of similarity in their respective pre-edge features and rising-edge energy positions, indicating practically identical Cu effective nuclear charges and ligand fields. The first electric-dipole-allowed Cu 1s \rightarrow 4p transitions at 8982.2 and 8982.5 eV in **1** and **2**, respectively, are well-resolved from the rising-edge features, which is indicative of a trigonal planar coordination geometry.¹⁵ The small shift of 0.3 eV upon oxidation of **1** indicates that **1** and **2** have similar effective oxidation states that are closer to cuprous than cupric when compared to the reference spectra for CuCl and CuCl₂ (Figure 2A).

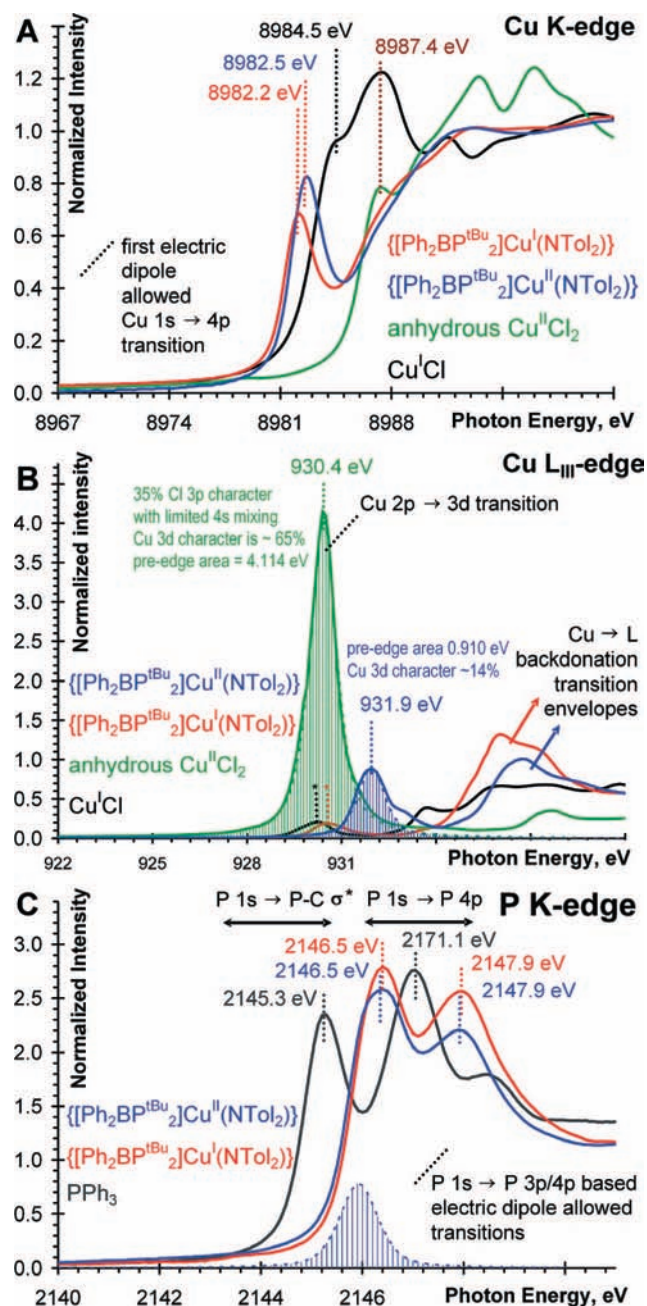


Figure 2. (A) Cu K-edge spectra, (B) Cu L_{III}-edge spectra, and (C) P K-edge spectra of CuCl (black), **1** (red), CuCl₂ (green), **2** (blue), and PPh₃ (gray). * = trace impurity.

Cu L-edge XAS was used to directly probe the Cu 3d character of the frontier orbitals in **1** and **2**. Figure 2B compares a set of features observed at the L₃ edge for complexes **1**, **2**, CuCl, and CuCl₂. The intense pre-edge feature at 930.4 eV for CuCl₂ is due

to the transition of a Cu 2p electron to the unoccupied Cu 3d-based LUMO. The Cu 3d character of the LUMO is determined to be about 65% on the basis of the area under this pre-edge feature.¹⁶ This intense feature disappears in the spectrum of CuCl.¹⁷ The group of features between 936 and 937 eV in the spectrum of **1** arise from Cu \rightarrow L back-donation. Similar but more intense features have been observed for dinuclear Cu–amidophosphine complexes.¹² Upon oxidation to **2**, a new feature at 931.9 eV appears, consistent with an electron being removed from an orbital with Cu 3d character. The proportion between the area of this feature and that of the pre-edge feature in CuCl₂ indicates that the redox-active molecular orbital in **2** has ~14% 3d character and therefore that the remainder of the electron density has to be ligand-centered.

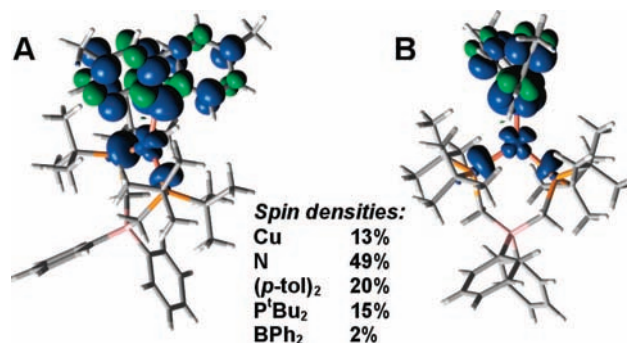


Figure 3. Atomic spin density plots¹⁸ (0.002 isocontours) for $\{[\text{Ph}_2\text{BP}^{\text{tBu}}]_2\text{Cu}(\text{NTol}_2)\}$ viewed (A) parallel and (B) perpendicular to the P₂CuN plane.

To dissect the role of the phosphine ligands in the redox process, we collected P K-edge XAS data (Figure 2C). In comparison with the PPh₃ reference spectra, the spectra of **1** and **2** are shifted toward higher energy because of an increase in P effective nuclear charge for the phosphines involved in P \rightarrow Cu donation. Upon oxidation, an electron hole is created in an orbital that has ~20% phosphorus character.¹⁶ This result and the 14% Cu 3d character clearly indicate that close to 70% of the redox-active frontier orbital of **1** and **2** must have N, C, and H character. This estimate is in good agreement with spin densities calculated using density functional theory (DFT),¹⁸ which indicate 13% unpaired spin character on Cu, 49% on N, 15% on P, and 20% on C/H of the *p*-tolyl groups (see Figure 3 for spin density plots).

Electron paramagnetic resonance (EPR) spectra of **2** were collected at the S, X, and Q bands (Figure 4A) and are quite unusual compared with those of typical cupric complexes. The S- and X-band spectra are dominated by six lines, each with several shoulders, unlike the typical four-line pattern expected for a single cupric center. Approximate simulations were obtained using the following parameters: (g_x, g_y, g_z) = (2.008, 2.008, 2.030); ($A_x^{\text{Cu}}, A_y^{\text{Cu}}, A_z^{\text{Cu}}$) = (34, 34, 170 MHz); ($A_x^{\text{P}}, A_y^{\text{P}}, A_z^{\text{P}}$) = (148, 148, 173 MHz); and ($A_x^{\text{N}}, A_y^{\text{N}}, A_z^{\text{N}}$) = (24, 100, 24 MHz).¹⁶ Though the simulation parameters are consistent with but not proof of experimental EPR parameters, reasonable fits were obtained using the same parameters at all three bands (Figures S10–S12), lending weight to their assignments. For comparison, one of Tolman's (β -diketiminato)Cu^{II}Cl complexes, a more typical three-coordinate Cu^{II} complex, has the parameters $g_{\parallel} = 2.20$, $g_{\perp} = 2.05$, $A_{\parallel}^{\text{Cu}} = 398$ MHz, $A_{\perp}^{\text{Cu}} = 52$ MHz.⁷ An example of a typical nitrogen radical is di-*t*-butylnitroxide (DTBN), which exhibits anisotropic hyperfine tensor components of $A^{\text{N}} = 89.6, 16.7, \text{ and } 21.3$ MHz.¹⁹ The comparatively small A^{Cu} and large A_y^{N} values in **2**, as well as the proximity of g_{average} for **2** to the value for the free electron, indicate a significant degree of spin delocalization between the Cu and N centers.

The XAS, DFT, and EPR analyses collectively suggest that **2** is better considered as a Cu^I-aminyl radical than a Cu^{II}-amido complex. This unusual electronic structure is also manifested in the chemical reactivity of the system. For instance, the addition of a H-atom donor such as Bu₃SnH, PhSH, or 9,10-dihydroanthracene to a solution of **2** cleanly produced [Ph₂BP^tBu₂]Cu(NHTol₂) (**3**). The byproducts Bu₃Sn-SnBu₃, PhS-SPh, and anthracene were detected by ¹H NMR spectroscopy and GC-MS, and the presence of an N-H linkage in **3** was confirmed by ¹H NMR [$\delta(\text{N-H}) = 4.93$ ppm] and IR spectroscopy [$\nu(\text{N-H}) = 3405$ cm⁻¹]. The hydrogen-atom transfer (HAT) reactivity of **2** is to our knowledge unprecedented for the formal Cu^{II} oxidation state. Instead, HAT reactions have been observed at Cu^{III} centers²⁰ or alternatively at Cu^{II}-aryloxy radicals.²¹ The reaction between **2** and either Bu₃SnD or Bu₃SnH provided a kinetic deuterium isotope effect of $k_{\text{H}}/k_{\text{D}} = 4.8(6)$ at room temperature. This value is more consistent with a concerted hydrogen-atom abstraction mechanism than with rate-limiting ET followed by proton transfer, and it is within the range observed for other Cu-containing systems.²¹

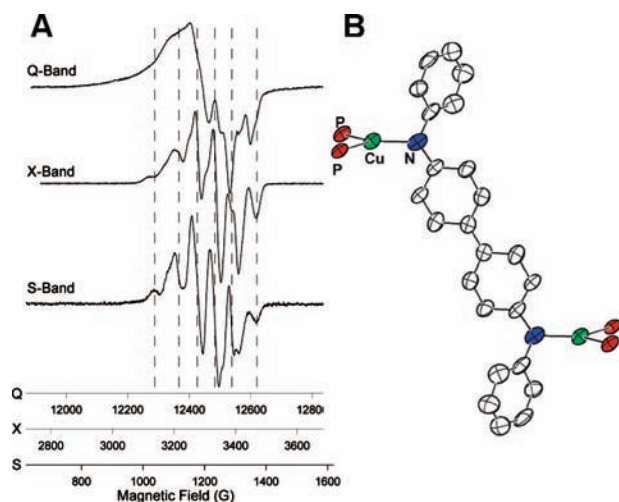


Figure 4. (A) Multifrequency EPR spectra of **2** recorded in a frozen dichloromethane/toluene glass. Microwave frequency (temperature): 35.100 GHz (123 K), 9.188 GHz (77 K), and 3.392 GHz (123 K) for the Q, X, and S bands, respectively. (B) Core structure of **5**, with only the phosphorus atoms of [Ph₂BP^tBu₂] shown.

A further indication of radical character delocalized into the aromatic rings in **2** comes from the oxidation chemistry of {[Ph₂BP^tBu₂]Cu(NPh)₂} {Li(12-crown-4)₂} (**4**), which lacks methyl groups para to the amido nitrogen. The reaction between **4** and [FeCp₂][PF₆] produces a bright-red diamagnetic dicopper product **5** in which two diphenylamido groups have been fused together at the positions para to the N atoms (Figure 4B; also see Figure S4). The identity of **5** was established using a relatively low quality X-ray crystal structure. Nonetheless, the short length of the new C-C bond [1.399(23) Å] in **5** and the planar geometries at these carbons indicate that 2 equiv of H atoms were lost subsequent to C-C coupling. Similar ligand-centered radical coupling has been observed in an oxidized Cu₂(μ-NR₂)₂ complex¹² and from a putative three-coordinate Cu^{II}-aryloxy intermediate generated by Tolman.⁷

In conclusion, we have isolated and thoroughly characterized a highly covalent, three-coordinate Cu-NAr₂ system in two distinct oxidation states, with the unusual oxidized form being best regarded as an aminyl radical ligated to Cu^I. Chemical reactivity facilitated by this electronic structure includes HAT, C-C coupling, and

efficient ET, the last being reminiscent of that in protein active sites bearing similar Cu coordination geometries.

Acknowledgment. This work was generously supported by the NSF (CHE-0750234; J.C.P.), the ONR (N00014-06-1016; R.K.S.), and the National Biomedical ESR Center Grant EB001980 from the NIH (W.E.A.). N.P.M. is grateful for an NSF graduate research fellowship. Portions of this research were carried out at the Stanford Synchrotron Radiation Lightsource, a national user facility operated by Stanford University on behalf of the U.S. DOE. The SSRL Structural Molecular Biology Program is supported by the DOE, Office of Biological and Environmental Research, and by the NIH, National Center for Research Resources, Biomedical Technology Program.

Supporting Information Available: Synthetic, spectroscopic, computational, and EPR simulation details; ET and HAT kinetics measurements; and Cu K-, Cu L-, and P K-edge data and fits. This material is available free of charge via the Internet at <http://pubs.acs.org>.

References

- (1) (a) Vallee, B. L.; Williams, R. J. P. *Proc. Natl. Acad. Sci. U.S.A.* **1968**, *59*, 498. (b) Gray, H. B.; Malmström, B. G. *Comments Inorg. Chem.* **1983**, *2*, 203.
- (2) (a) Ducros, V.; Brzozowski, A. M.; Wilson, K. S.; Brown, S. H.; Ostergaard, P.; Schneider, P.; Yaver, D. S.; Pederson, A. H.; Davies, G. J. *Nat. Struct. Biol.* **1998**, *5*, 310. (b) Zaitseva, I.; Zaitsev, V.; Card, G.; Moshkov, K.; Bax, B.; Ralph, A.; Lindley, P. J. *Biol. Inorg. Chem.* **1996**, *1*, 15. (c) Karlsson, B. G.; Nordling, M.; Pascher, T.; Tsai, L.-C.; Sjölin, L.; Lundberg, L. G. *Protein Eng.* **1991**, *4*, 343.
- (3) Rorabacher, D. B. *Chem. Rev.* **2004**, *104*, 651.
- (4) (a) Marcus, R. A.; Sutin, N. *Biochim. Biophys. Acta* **1985**, *2*, 203. (b) Gray, H. B.; Malmström, B. G.; Williams, R. J. P. *J. Biol. Inorg. Chem.* **2000**, *5*, 551.
- (5) Selected examples: (a) Chaka, G.; Sonneberg, J. L.; Schlegel, H. B.; Heeg, M. J.; Jaeger, G.; Nelson, T. J.; Ochrymowycz, L. A.; Rorabacher, D. B. *J. Am. Chem. Soc.* **2007**, *129*, 5217. (b) Fujisawa, K.; Fujita, K.; Takahashi, T.; Kitajima, N.; Moro-oka, Y.; Matsunaga, Y.; Miyashita, Y.; Okamoto, K. *Inorg. Chem. Commun.* **2004**, *7*, 1188.
- (6) Mankad, N. P.; Peters, J. C. *Chem. Commun.* **2008**, 1061.
- (7) (a) Jazdzewski, B. A.; Holland, P. L.; Pink, M.; Young, V. G., Jr.; Spencer, D. J. E.; Tolman, W. B. *Inorg. Chem.* **2001**, *40*, 6097. (b) Holland, P. L.; Tolman, W. B. *J. Am. Chem. Soc.* **1999**, *121*, 7270.
- (8) A subset of the β-diketiminato copper(II) system studied by Tolman does access reversible one-electron chemistry by cyclic voltammetry, but syntheses of the corresponding copper(I) complexes have not been reported. See ref 7.
- (9) Harkins, S. B.; Peters, J. C. *J. Am. Chem. Soc.* **2004**, *126*, 2885.
- (10) (a) Gamelin, D. R.; Randall, D. W.; Hay, M. T.; Houser, R. P.; Mulder, T. C.; Canters, G. W.; de Vries, S.; Tolman, W. B.; Lu, Y.; Solomon, E. I. *J. Am. Chem. Soc.* **1998**, *120*, 5246. (b) DeBeer-George, S.; Metz, M.; Szilagy, R. K.; Wang, J.; Cramer, S. P.; Lu, Y.; Tolman, W. B.; Hedman, B.; Hodgson, K. O.; Solomon, E. I. *J. Am. Chem. Soc.* **2001**, *123*, 5757.
- (11) (a) Solomon, E. I.; Randall, D. W.; Glaser, T. *Coord. Chem. Rev.* **2000**, *200-202*, 595. (b) Szilagy, R. K.; Solomon, E. I. *Curr. Opin. Chem. Biol.* **2002**, *6*, 250.
- (12) Harkins, S. B.; Mankad, N. P.; Miller, A. J. M.; Szilagy, R. K.; Peters, J. C. *J. Am. Chem. Soc.* **2008**, *130*, 3478.
- (13) Büttner, T.; Geier, J.; Frison, G.; Harmer, J.; Calle, C.; Schweiger, A.; Schönberg, H.; Grützmacher, H. *Science* **2005**, *307*, 235.
- (14) For a brief review, see: Hicks, R. G. *Angew. Chem., Int. Ed.* **2008**, *47*, 2. Also see: Miyazato, Y.; Wada, T.; Muckerman, J. T.; Fujita, E.; Tanaka, K. *Angew. Chem., Int. Ed.* **2007**, *46*, 5728.
- (15) Kau, L. S.; Spira-Solomon, D. J.; Pennerhahn, J. E.; Hodgson, K. O.; Solomon, E. I. *J. Am. Chem. Soc.* **1987**, *109*, 6433.
- (16) See the Supporting Information for details.
- (17) The small features (* in Figure 2) at 930.3 and 930.7 eV for CuCl and complex **1**, respectively, are due to contamination from oxidation during shipping and handling.
- (18) The B(38HF)P86 functional and GT-6-311+G(d) basis set were employed. Spin densities were estimated using Mulliken population analysis.
- (19) Libertint, L. J.; Griffith, O. H. *J. Chem. Phys.* **1970**, *53*, 1359.
- (20) Lockwood, M. A.; Blubaugh, T. J.; Collier, A. M.; Lovell, S.; Mayer, J. M. *Angew. Chem., Int. Ed.* **1999**, *38*, 225.
- (21) Selected examples: (a) Thomas, F.; Gellon, G.; Gautier-Luneau, I.; Saint-Aman, E.; Pierre, J.-L. *Angew. Chem., Int. Ed.* **2002**, *41*, 3047. (b) Chaudhuri, P.; Hess, M.; Weyhermüller, T.; Wieghardt, K. *Angew. Chem., Int. Ed.* **1999**, *38*, 1095. (c) Wang, Y.; DuBois, J. L.; Hedman, B.; Hodgson, K. O.; Stack, T. D. P. *Science* **1998**, *279*, 537.

JA809834K